ACS APPLIED MATERIALS & INTERFACES

Research Article

www.acsami.org

Novel Carbazole-Based Hole-Transporting Materials with Star-Shaped Chemical Structures for Perovskite-Sensitized Solar Cells

Min Soo Kang,[†] Sang Do Sung,[§] In Taek Choi,[†] Hyoungjin Kim,[‡] MunPyo Hong,[‡] Jeongho Kim,[§] Wan In Lee,*[,§] and Hwan Kyu Kim*[,†]

[†]Global GET-Future Laboratory & Department of Advanced Materials Chemistry and [‡]Department of Display & Semiconductor Physics, Korea University, 2511 Sejong-ro, Jochiwon, Sejong 339-700, Korea

[§]Department of Chemistry and Chemical Engineering, Inha University, Incheon 402-751, Korea

Supporting Information

ABSTRACT: Novel carbazole-based hole-transporting materials (HTMs), including extended π-conjugated central core units such as 1,4-phenyl, 4,4′-biphenyl, or 1,3,5-trisphenylbenzene for promoting effective $\pi-\pi$ stacking as well as the hexyloxy flexible group for enhancing solubility in organic solvent, have been synthesized as HTM of perovskite-sensitized solar cells. A HTM with 1,3,5-trisphenylbenzene core, coded as **SGT-411**, exhibited the highest charge conductivity caused by its intrinsic property to form crystallized structure. The perovskite-sensitized solar cells with **SGT-411** exhibited the highest PCE of 13.00%, which is 94% of that of the device derived from *spiro*-OMeTAD (13.76%). Time-resolved photoluminescence spectra indicate that **SGT-411** shows the shortest decay time constant, which is in agreement with the trends of conductivity data, indicating it having fastest charge regeneration. In this regard, a carbazole-based HTM with star-shaped chemical structure is considered to be a promising candidate HTM.

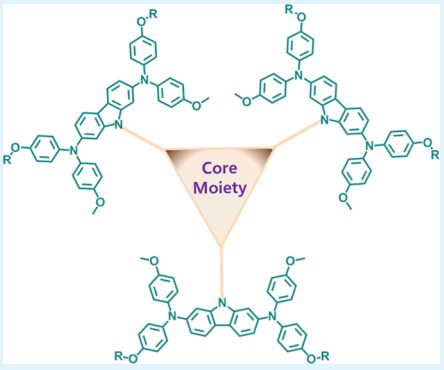

KEYWORDS: *perovskite-sensitized solar cells, hole-transporting materials, carbazole, star-shaped chemical structures, charge-transfer efficiency*

INTRODUCTION

Since solid-state dye-sensitized solar cells (ssDSSCs) were introduced in 1998 by Bach and Grätzel,[1,2] in which the liquid electrolyte was replaced by an organic hole-transport material (HTM) such as 2,2′,7,7′-tetrakis(N,N-p-dimethoxy-phenyl-amino)-9,9′-*spiro*bifluorene (*spiro*-OMeTAD), the efficiency of *spiro*-OMeTAD-based ssDSSCs has increased dramatically through dye development. The highest recorded efficiency of 7.2% was achieved by using a Y123 organic dye with a high molar extinction coefficient.[3−11] Recently, methylammonium lead halide ($CH_3NH_3PbX_3$, in which X corresponds to a halogen) perovskites have been introduced as promising light harvesters in solar cells, leading to power conversion efficiencies (PCEs; η) exceeding 15% when used in combination with *spiro*-OMeTAD under 1 sun (100 mW cm^{-2}) illumination.[12−17] However, the spirobifluorene core of *spiro*-OMeTAD is relatively expensive, owing to the multistep processes required for its preparation. Therefore, it is of importance to develop more economical alternatives to *spiro*-OMeTAD for the successful commercialization of hybrid perovskite solar cells.

From this perspective, Seok and co-workers reported an energy conversion efficiency of 12.4% with pyrene-core arylamine derivatives (PY-C) in hybrid perovskite-sensitized solar cells.[18] Recently, Ma et al. reported an energy conversion efficiency of 7.1% with triphenylamine derivatives (TPD) in hybrid perovskite-sensitized solar cells. Moreover,[19] Li et al. reported a 13.8% conversion efficiency with a simple HTM of 2,5-bis(4,4′-bis(methoxyphenyl)aminophen-4″-yl)-3,4-ethylenedioxyth-iophene, and this is one of the highest PCE values reported to date for $TiO_2/CH_3NH_3PbI_3$ perovskite/small-molecule HTMs, with the exception of *spiro*-OMeTAD.[20]

HTMs based on the carbazole moiety have been the subject of an increasing number of investigations over the past decade. This could be explained by their interesting features such as the low cost of the 9H-carbazole starting material, good chemical and environmental stability provided by the fully aromatic unit, as well as easy incorporation of a wide variety of functional groups into the nitrogen atom that allow better solubility and fine-tuning of the electronic and optical properties. In 2011, Leijtens et al. designed a new HTM (AS 44), in which the central 2,7-fluorene core in *spiro*-OMeTAD were replaced by a more electron-donating N-hexyl-2,7-carbazole core, with high solubility to improve pore filling into mesoporous titania films.[21] By using Z907 as the sensitizing dye in a DSSC, the cell based on this HTM achieved the best efficiency of 2.94% when using a 2 μm thick TiO_2 film, rivalling the efficiency of

Received: May 28, 2015
Accepted: September 9, 2015
Published: September 9, 2015

DOI: 10.1021/acsami.5b04662
ACS Appl. Mater. Interfaces 2015, 7, 22213−22217

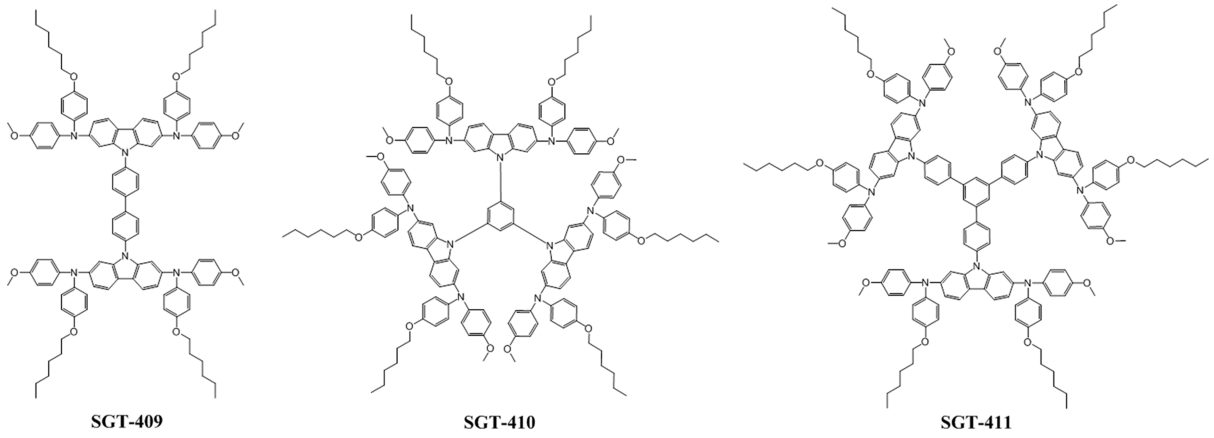

Figure 1. Chemical structures of the new HTMs synthesized and used in this work.

conventional *spiro*-OMeTAD-based cells. This photovoltaic performance surpassed that of the *spiro*-OMeTAD cell, even when its TiO_2 thickness was increased to 6 μm, which highlights its promising application in high-efficiency ssDSSCs. Puckyte et al. also reported a 3.44% energy conversion efficiency with a new HTM based on a carbazole moiety substituted with bis(4-methoxy-phenyl)-amine using D102 organic dye, indicating that carbazole derivatives are promising candidates for the replacement of *spiro*-OMeTAD.[22]

In our previous work, we reported the synthesis and characterization of novel carbazole-based HTMs with two- or three-armed chemical structures, which were linked through phenylene-derived central core units. We also investigated their application in $CH_3NH_3PbX_3$-based perovskite-sensitized solar cells. A high PCE of 14.79%, which is comparable to that of the device with a commercial *spiro*-OMeTAD (15.23%), was achieved with the three-armed SGT-405 HTM that possessed partial crystalline properties, and we also demonstrated that the charge conductivity of HTMs is a major factor determining the cell performance of perovskite-sensitized solar cells.[23] In this work, we report the design of further carbazole-based HTMs that include extended π-conjugated central core units, such as 1,4-phenyl, 4,4′ biphenyl, or 1,3,5-trisphenylbenzene core unit for promoting effective $\pi-\pi$ stacking, and a flexible hexyloxy group that enhances solubility in organic solvents used to fabricate perovskite-sensitized solar cells.

Furthermore, we first synthesized several HTMs, introducing extended π-conjugated central core units, including those with only a methoxy group at the electron-donating diarylamine position to promote $\pi-\pi$ stacking for efficient charge transport between the HTM molecules. However, the solubility of the resultant HTMs in chlorobenzene, which is conventionally used as a solvent to prepare the spin-coating solution, was very poor, owing to their rigid chemical structures. Thus, a flexible hexyloxy group is also introduced instead of the methyl group, and the materials were coded as **SGT-409**, **SGT-410**, and **SGT-411** (Figure 1).

RESULTS AND DISCUSSION

UV/vis absorption spectra of the newly synthesized HTMs and *spiro*-OMeTAD dissolved in THF are shown in Figure 2. The determined molar absorption coefficients (ε) as well as the absorption maxima are listed in Table 1. The synthesized HTMs showed only slight differences in their absorption maxima (389 nm for **SGT-409**, 393 nm for **SGT-410**, and 387 nm for **SGT-411**) compared to that of *spiro*-OMeTAD at 386 nm (see Table 1). The new two-armed **HTM SGT-409** exhibited the smallest molar extinction coefficient among the new HTMs, which was similar to that of *spiro*-OMeTAD and was considered to be a favorable HTM property because loss of solar light through absorption of the HTM can be minimized, whereas **SGT-410** and **SGT-411**, possessing three-armed (or star-shaped) chemical structures, exhibited higher molar extinction coefficients as a result of the increasing number of the hole-transporting moieties.

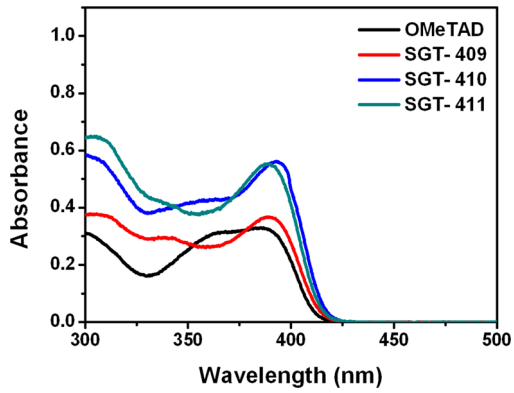

Figure 2. UV/vis absorption spectra of various HTMs dissolved in THF.

The band gap energies were determined to be 3.02 eV for **SGT-409**, 2.99 eV for **SGT-410**, and 3.00 eV for **SGT-411**, which are very close to that of *spiro*-OMeTAD. The oxidation potentials of the synthesized HTMs as well as that of commercial *spiro*-OMeTAD were measured by using cyclic voltammetry, as shown in Figure S1 and in Table 1. The HOMO energy levels were derived from the first oxidation potential, whereas the LUMO energy levels were determined by subtracting the band gap energies from the HOMO energy levels of the HTMs. The HOMO levels of new HTMs (0.73 V vs NHE for **SGT-409**, 0.75 V vs NHE for **SGT-410**, and 0.72 V vs NHE for **SGT-411**) are close to that of *spiro*-OMeTAD (0.73 V vs NHE), suggesting that the energy levels of the synthesized HTMs are suitable for effective transport of holes from the $CH_3NH_3PbI_3$ layer.

Thermal analysis was conducted through thermogravimetric analysis (TGA) and differential scanning calorimetry (DSC) measurements. Each of the new HTMs began to decompose at approximately 400 °C. According to DSC analysis, only **SGT-**

DOI: 10.1021/acsami.5b04662
ACS Appl. Mater. Interfaces 2015, 7, 22213−22217

Table 1. Photophysical, Electrochemical, and Photovoltaic Performance Data of Perovskite Solar Cells Employing New HTMs and a Measurement Condition of 3 V S^{-1}

		potentials and energy level			photovoltaic performance data			
HTMs	absorption λ_{max} (nm) (ε ($M^{-1}cm^{-1}$))[a]	E_{ox} (V vs NHE)[b]	E_{0-0} (V vs NHE)[c]	$E_{ox} - E_{0-0}$ (V vs NHE)	J_{sc} (mA cm^{-2})	V_{oc} (V)	FF (%)	η (%)
SGT-409	389 (73380)	0.73	3.02	−2.29	18.63	0.938	62.65	10.96
SGT-410	393 (100350)	0.75	2.99	−2.24	18.55	0.984	67.2	12.61
SGT-411	387 (110280)	0.72	3.00	−2.28	18.60	0.997	67.2	13.00
spiro-OMeTAD					18.82	1.011	67.49	13.76

[a]Absorption and emission spectra were measured in THF solution. [b]The oxidation potentials of dyes were measured in THF with 0.1 M tetrabutylammonium hexafluorophosphate ($TBAPF_6$) with a scan rate of 50 mV s^{-1} (vs NHE) with the ferrocene/ferrocenium standard. [c]E_{0-0} was determined from the onset of absorption spectra.

411 showed a melting temperature (T_m) of 218 °C, exhibiting its intrinsic property to form a crystalline structure. The other HTMs showed no T_m, indicating an amorphous structure (Figure S2). Interestingly, **SGT-410**, which is a derivative of previously reported **SGT-405**,[24] lost its T_m by substituting a methoxy group with a flexible hexyloxy group, whereas **SGT-411** with an extended π-conjugated central core unit, still exhibited a sharp T_m, indicating its partial crystallinity despite the introduction of the flexible hexyloxy group.

Figure 3 shows the current−voltage (I−V) characteristics for in-plane hole-only devices based on several HTMs. We

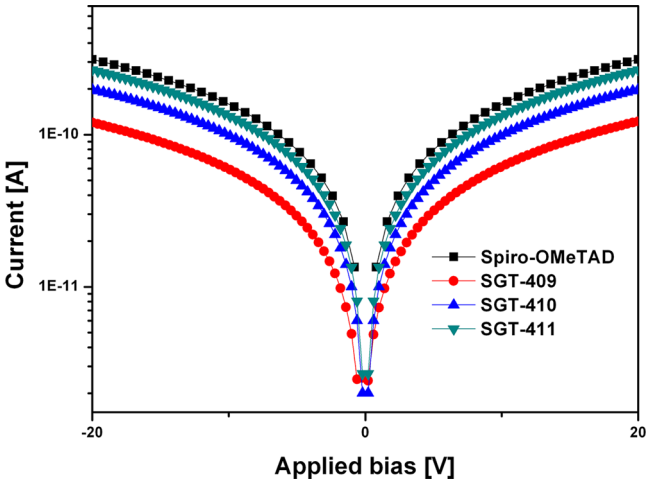

Figure 3. I−V characteristics of the in-plane devices employing various HTMs, spin-coated with a 5 wt % toluene solution.

observed straight lines for all curves (when plotted in a linear scale), implying ohmic contact between the gold and the HTM layers.[24] The conductivity (σ) was determined by using eq 1,[24] in which L is the channel length (100 μm), w is the channel width (500 μm), t is the film thickness (410 nm for **SGT-409**, 390 nm for **SGT-410** and 460 nm for **SGT-411**), and R is the resistivity calculated from the gradients of the curves.

$$\sigma = L/Rwt \quad (1)$$

The obtained conductivities for **SGT-409**, **SGT-410**, and **SGT-411** were 3.0×10^{-9}, 5.1×10^{-8} and 5.8×10^{-8} S cm^{-1}, respectively. Among the three HTMs, **SGT-410** and **SGT-411**, with three-armed chemical structures, exhibited a relatively higher conductivity than the two-armed HTM **SGT-409**. Also, it was demonstrated that **SGT-411**, with its π-extended central core, possesses a reproducible T_m, indicating its partial crystallinity, and shows the highest σ value, which was close to that of *spiro*-OMeTAD (6.4×10^{-8} S cm^{-1}).[24] This result is consistent that of our previous report on carbazole-based HTMs with a three-armed chemical structure; therefore, the three-armed chemical structures seem to be more promising scaffolds in designing HTMs with high charge conductivity. In addition, we also reported that the reproducible T_m in the three-armed chemical structures originated from its unique property to form a crystallized structure, which probably plays an important role in increasing charge conductivity.

Figure 4 shows the J−V curves (Figure 4a) and IPCE spectra (Figure 4b) of the perovskite-sensitized solar cells employing

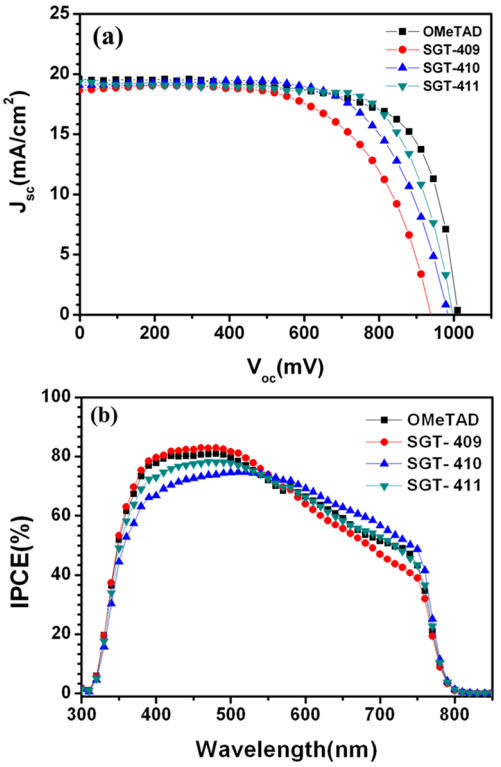

Figure 4. (a) J−V curves and (b) IPCE spectra of the perovskite solar cells employing various HTMs.

various HTMs. The synthesized SGT series was then applied as HTM layers in $CH_3NH_3PbI_3$-based perovskite solar cells. The J−V curves of the perovskite-sensitized solar cells, derived from the **SGT-409** (Cell-409), **SGT-410** (Cell-410), **SGT-411** (Cell-411), and *spiro*-**OMETAD** (Cell-S), are shown in Figure 4a, whereas the detailed J−V parameters are listed in Table 1. Among the three perovskite cells derived from the **SGT** series, the cell derived from **SGT-411** (Cell-411) exhibited the highest

DOI: 10.1021/acsami.5b04662
ACS Appl. Mater. Interfaces 2015, 7, 22213−22217

PCE (13.00%) with a short-circuit current density (J_{SC}) of 19.31 mA cm^{-2}, open-circuit voltage (V_{OC}) of 997 mV, and a fill factor (*FF*) of 67.49. Interestingly, the V_{OC} values decreased on the order of Cell-411, Cell-410, and Cell-409, whereas the J_{SC} values did not vary appreciably. The obtained results suggest that the trend of V_{OC} values is closely related to the charge conductivity of the employed HTM, which is consistent with our previous report. Previously, we reported that as the conductivity of the HTM decreases the hole-transport rate from $CH_3NH_3PbI_3$ to the HTM and the recombination rate of photoexcited electrons in $CH_3NH_3PbI_3$ is expedited thus leading to a decrease in V_{OC}. Compared with the cell derived from *spiro*-OMeTAD (Cell-S), which exhibited a PCE of 13.76% with a J_{SC} of 19.58 mA cm^{-2}, a V_{OC} of 1011 mV, and a *FF* of 69.48, Cell-411 was quite similar in terms of the J_{SC}, but the V_{OC} and *FF* were slightly lower; this is also expected to be caused by the relatively low charge conductivity of **SGT-411** compared to that of *spiro*-OMeTAD. The incident photon-to-current conversion efficiency (IPCE) spectra of the perovskite cells are shown in Figure 4b. The integrated current densities estimated from the total areas of the IPCE spectra were in good agreement with the J_{SC} values acquired from the $J-V$ curves. When employing the new HTMs, the devices induce the highest quantum efficiency over the entire spectral region, with a maximum external quantum efficiency (EQE) of about 80%, which is comparable to the EQE of the device employing *spiro*-OMeTAD.

To evaluate the efficiency of charge transfer from the perovskite to the HTM, we measured time-resolved photoluminescence (TR-PL) of HTM/$CH_3NH_3PbI_3$/Pyrex glass devices, which employ various HTMs, as can be seen in Figure 5. The TR-PL decay of these perovskite devices can arise from

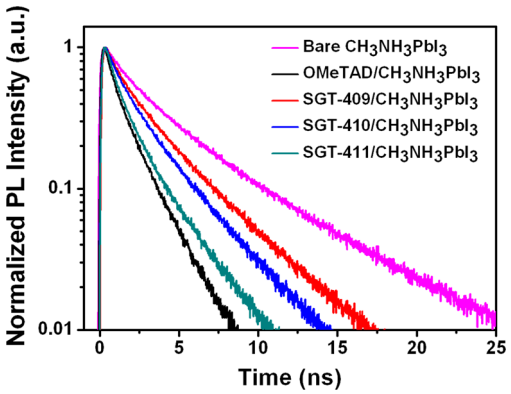

Figure 5. PL decay curves of bare $CH_3NH_3PbI_3$ and HTM/$CH_3NH_3PbI_3$/Pyrex glass devices employing various HTMs. It can clearly be seen that the TR-PL decay becomes faster in the order of bare $CH_3NH_3PbI_3$, **SGT-409**, **SGT-410**, **SGT-411**, and *spiro*-OMeTAD.

quenching of the PL intensity, owing to either (1) radiative recombination of excited electrons and holes in the perovskite material or (2) hole transport from the perovskite to the HTM.

The rate of radiative recombination of electrons and holes can be obtained from the TR-PL decay of bare $CH_3NH_3PbI_3$, for which the time constant was 3.9 ns, as shown in Table 2. With HTMs present in the devices, the TR-PL decay is accelerated, owing to hole injection from the perovskite to the HTM. In particular, the time constant ($\tau_{interface}$) for the TR-PL decay of the devices becomes smaller upon changing the HTM,

Table 2. Charge-Transfer Time (τ_{CT}) and Charge-Transfer Efficiency (CTE) Calculated from the PL Lifetimes ($\tau_{interface}$) of HTM/$CH_3NH_3PbI_3$/Pyrex Glass Devices Employing Various HTMs

HTM	$\tau_{interface}$ (ns)[a]	τ_{CT} (ns)	CTE (%)
bare $CH_3NH_3PbI_3$	3.9 ± 0.1[b]		
SGT-409/$CH_3NH_3PbI_3$	2.2 ± 0.1	5.1	43.2
SGT-410/$CH_3NH_3PbI_3$	1.8 ± 0.1	3.5	52.6
SGT-411/$CH_3NH_3PbI_3$	1.2 ± 0.1	1.8	68.5
spiro-OMeTAD/$CH_3NH_3PbI_3$	1.0 ± 0.1	1.3	74.8

[a]The PL lifetime of each $CH_3NH_3PbI_3/TiO_2$/Pyrex glass sample corresponds to the amplitude-weighted average lifetime of a multi-exponential decay fit. [b]Time constant for the TR-PL decay of the bare $CH_3NH_3PbI_3$ film.

following the order of **SGT-409** > **SGT-410** > **SGT-411** > *spiro*-OMeTAD. By using the relationship of $1/\tau_{interface} = 1/\tau_{perovskite} + 1/\tau_{CT}$, we calculated charge-transfer time (τ_{CT}) and charge-transfer efficiency (CTE = $k_{CT}/k_{interface} = \tau_{interface}/\tau_{CT}$) for each device, as listed in Table 2. The τ_{CT} values change according to the same trend as $\tau_{interface}$, whereas the CTE values increase in the order of **SGT-409** < **SGT-410** < **SGT-411** < *spiro*-OMeTAD, which is in good agreement with the variation trend of photovoltaic efficiency. In summary, three novel carbazole-based HTMs have been synthesized and employed as HTMs in perovskite-sensitized solar cells. Among them, **SGT-411** exhibited the highest charge conductivity, which seems to be caused by its intrinsic property to form a crystallized structure during its fabrication. The perovskite-sensitized solar cell employing **SGT-411** exhibited the highest PCE of 13.00%, which is 94% of that of the device derived from the commercial *spiro*-OMeTAD material (13.76%). TR-PL spectra indicate that **SGT-411** shows the shortest decay time constant, which is in agreement with the trends of conductivity data, indicating that it had the fastest charge regeneration. Thus, it was demonstrated that the conductivity of a HTM is one of the essential factors in determining the efficiency of the perovskite-sensitized cell, which is consistent with our previous report. In this regard, a carbazole-based hole-transporting material with a star-shaped chemical structure is considered a promising candidate HTM.

CONCLUSIONS

Three novel carbazole-based HTMs have been synthesized and employed as HTMs in perovskite-sensitized solar cells. Among them, **SGT-411** exhibited the highest charge conductivity, which seems to be caused by its intrinsic property to form a crystallized structure during its fabrication. The perovskite-sensitized solar cell employing **SGT-411** exhibited the highest PCE of 13.00%, which is 94% of that of the device derived from the commercial *spiro*-OMeTAD material (13.76%). TR-PL spectra indicate that **SGT-411** shows the shortest decay time constant, which is in agreement with the trends of conductivity data, indicating that it had the fastest charge regeneration. Thus, it was demonstrated that the conductivity of a HTM is one of the essential factors in determining the efficiency of the perovskite cell, which is consistent with our previous report. In this regard, a carbazole-based hole-transporting material with a star-shaped chemical structure is considered a promising candidate HTM.

DOI: 10.1021/acsami.5b04662
ACS Appl. Mater. Interfaces 2015, 7, 22213−22217

■ ASSOCIATED CONTENT

Supporting Information

The Supporting Information is available free of charge on the ACS Publications website at DOI: 10.1021/acsami.5b04662.

(PDF)

■ AUTHOR INFORMATION

Corresponding Authors

*E-mail: wanin@inha.ac.kr.

*E-mail: hkk777@korea.ac.kr. Fax:+82-44-860-1331. Tel.: +82-44- 860-1493.

Author Contributions

M.S.K. and S.D.S. contributed equally to this work.

Notes

The authors declare no competing financial interest.

■ ACKNOWLEDGMENTS

This work was supported by a National Research Foundation of Korea (NRF) grant funded by the Korean government (MSIP) (no. 2014R1A2A1A10051630), the International Collaborative Energy Technology R&D Program of the Korean Institute of Energy Technology Evaluation and Planning (KETEP) granted financial resource from the Ministry of Trade, Industry & Energy, Republic of Korea (no. 20148520011250).

■ REFERENCES

(1) Mathew, S.; Yella, A.; Gao, P.; Humphry-Baker, R.; Curchod, B. F. E.; Ashari-Astani, N.; Tavernelli, I.; Rothlisberger, U.; Nazeeruddin, Md. K.; Grätzel, M. Dye-sensitized solar cells with 13% efficiency achieved through the molecular engineering of porphyrin sensitizers. *Nat. Chem.* **2014**, *6* (3), 242−247.

(2) Grätzel, M.; Bach, U.; Lupo, D.; Comte, P.; Moser, J. E.; Weissortel, F.; Salbeck, J.; Spreitzer, H. Solid-state dye-sensitized mesoporous TiO2 solar cells with high photon-to-electron conversion efficiencies. *Nature* **1998**, *395* (6702), 583−585.

(3) Burschka, J.; Dualeh, A.; Kessler, F.; Baranoff, E.; Cevey-Ha, N.-L.; Yi, C.; Nazeeruddin, M. K.; Grätzel, M. Tris(2-(1H-pyrazol-1-yl)pyridine)cobalt(III) as p-Type Dopant for Organic Semiconductors and Its Application in Highly Efficient Solid-State Dye-Sensitized Solar Cells. *J. Am. Chem. Soc.* **2011**, *133* (45), 18042−18045.

(4) Schmidt-Mende, L.; Bach, U.; Humphry-Baker, R.; Horiuchi, T.; Miura, H.; Ito, S.; Uchida, S.; Grätzel, M. Organic Dye for Highly Efficient Solid-State Dye-Sensitized Solar Cells. *Adv. Mater.* **2005**, *17* (7), 813−815.

(5) Snaith, H. J.; Petrozza, A.; Ito, S.; Miura, H.; Grätzel, M. Charge Generation and Photovoltaic Operation of Solid-State Dye-Sensitized Solar Cells Incorporating a High Extinction Coefficient Indolene-Based Sensitizer. *Adv. Funct. Mater.* **2009**, *19* (11), 1810−1818.

(6) Moon, S.-J.; Yum, J.-H.; Humphry-Baker, R.; Karlsson, K. M.; Hagberg, D. P.; Marinado, T.; Hagfeldt, A.; Sun, L.; Grätzel, M.; Nazeeruddin, M. K. Highly Efficient Organic Sensitizers for Solid-State Dye-Sensitized Solar Cells. *J. Phys. Chem. C* **2009**, *113* (38), 16816−16820.

(7) Kwon, Y. S.; Lim, J.; Song, I.; Song, I. Y.; Shin, W. S.; Moon, S.-J.; Park, T. Chemical compatibility between a hole conductor and organic dye enhances the photovoltaic performance of solid-state dye-sensitized solar cells. *J. Mater. Chem.* **2012**, *22* (17), 8641−8648.

(8) Jiang, X.; Karlsson, K. M.; Gabrielsson, E.; Johansson, E. M. J.; Quintana, M.; Karlsson, M.; Sun, L.; Boschloo, G.; Hagfeldt, A. Highly Efficient Solid-State Dye-Sensitized Solar Cells Based on Triphenylamine Dyes. *Adv. Funct. Mater.* **2011**, *21* (15), 2944−2952.

(9) Chen, D.-Y.; Hsu, Y.-Y.; Hsu, H.-C.; Chen, B.-S.; Lee, Y.-T.; Fu, H.; Chung, M.-W.; Liu, S.-H.; Chen, H.-C.; Chi, Y.; Chou, P.-T. Organic dyes with remarkably high absorptivity; all solid-state dye sensitized solar cell and role of fluorine substitution. *Chem. Commun.* **2010**, *46* (29), 5256−5258.

(10) Cai, N.; Moon, S.-J.; Cevey-Ha, L.; Moehl, T.; Humphry-Baker, R.; Wang, P.; Zakeeruddin, S. M.; Grätzel, M. An Organic D-π-A Dye for Record Efficiency Solid-State Sensitized Heterojunction Solar Cells. *Nano Lett.* **2011**, *11* (4), 1452−1456.

(11) Jang, S.-R.; Zhu, K.; Ko, M. J.; Kim, K.; Kim, C.; Park, N.-G.; Frank, A. J. Voltage-Enhancement Mechanisms of an Organic Dye in High Open-Circuit Voltage Solid-State Dye-Sensitized Solar Cells. *ACS Nano* **2011**, *5* (10), 8267−8274.

(12) Burschka, J.; Pellet, N.; Moon, S.-J.; Humphry-Baker, R.; Gao, P.; Nazeeruddin, M. K.; Gratzel, M. Sequential deposition as a route to high-performance perovskite-sensitized solar cells. *Nature* **2013**, *499* (7458), 316−319.

(13) Liu, M.; Johnston, M. B.; Snaith, H. J. Efficient planar heterojunction perovskite solar cells by vapour deposition. *Nature* **2013**, *501* (7467), 395−398.

(14) Ramos, F. J.; López-Santos, M. C.; Guillén, E.; Nazeeruddin, M. K.; Grätzel, M.; Gonzalez-Elipe, A. R.; Ahmad, S. Perovskite Solar Cells Based on Nanocolumnar Plasma-Deposited ZnO Thin Films. *ChemPhysChem* **2014**, *15* (6), 1148−1153.

(15) Noh, J. H.; Jeon, N. J.; Choi, Y. C.; Nazeeruddin, M. K.; Gratzel, M.; Seok, S. I. Nanostructured TiO2/CH3NH3PbI3 heterojunction solar cells employing spiro-OMeTAD/Co-complex as hole-transporting material. *J. Mater. Chem. A* **2013**, *1* (38), 11842−11847.

(16) Park, N.-G. Organometal Perovskite Light Absorbers Toward a 20% Efficiency Low-Cost Solid-State Mesoscopic Solar Cell. *J. Phys. Chem. Lett.* **2013**, *4* (15), 2423−2429.

(17) Kim, H.-S.; Lee, C.-R.; Im, J.-H.; Lee, K.-B.; Moehl, T.; Marchioro, A.; Moon, S.-J.; Humphry-Baker, R.; Yum, J.-H.; Moser, J. E.; Gratzel, M.; Park, N.-G. Lead Iodide Perovskite Sensitized All-Solid-State Submicron Thin Film Mesoscopic Solar Cell with Efficiency Exceeding 9%. *Sci. Rep.* **2012**, *2*, 591 DOI: 10.1038/srep00591.

(18) Jeon, N. J.; Lee, J.; Noh, J. H.; Nazeeruddin, M. K.; Grätzel, M.; Seok, S. I. Efficient Inorganic−Organic Hybrid Perovskite Solar Cells Based on Pyrene Arylamine Derivatives as Hole-Transporting Materials. *J. Am. Chem. Soc.* **2013**, *135* (51), 19087−19090.

(19) Ma, Y.; Chung, Y.-H.; Zheng, L.; Zhang, D.; Yu, X.; Xiao, L.; Chen, Z.; Wang, S.; Qu, B.; Gong, Q.; Zou, D. Improved Hole-Transporting Property via HAT-CN for Perovskite Solar Cells without Lithium Salts. *ACS Appl. Mater. Interfaces* **2015**, *7* (12), 6406−6411.

(20) Li, H.; Fu, K.; Hagfeldt, A.; Grätzel, M.; Mhaisalkar, S. G.; Grimsdale, A. C. A Simple 3,4-Ethylenedioxythiophene Based Hole-Transporting Material for Perovskite Solar Cells. *Angew. Chem., Int. Ed.* **2014**, *53* (16), 4085−4088.

(21) Leijtens, T.; Ding, I. K.; Giovenzana, T.; Bloking, J. T.; McGehee, M. D.; Sellinger, A. Hole Transport Materials with Low Glass Transition Temperatures and High Solubility for Application in Solid-State Dye-Sensitized Solar Cells. *ACS Nano* **2012**, *6* (2), 1455−1462.

(22) Puckyte, G.; Schmaltz, B.; Tomkeviciene, A.; Degbia, M.; Grazulevicius, J. V.; Melhem, H.; Bouclé, J.; Tran-Van, F. Carbazole-based molecular glasses for efficient solid-state dye-sensitized solar cells. *J. Power Sources* **2013**, *233* (0), 86−92.

(23) Sung, S. D.; Kang, M. S.; Choi, I. T.; Kim, H. M.; Kim, H.; Hong, M.; Kim, H. K.; Lee, W. I. 14.8% perovskite solar cells employing carbazole derivatives as hole transporting materials. *Chem. Commun.* **2014**, *50* (91), 14161−14163.

(24) Snaith, H. J.; Grätzel, M. Enhanced charge mobility in a molecular hole transporter via addition of redox inactive ionic dopant: Implication to dye-sensitized solar cells. *Appl. Phys. Lett.* **2006**, *89* (26), 262114.